Nonlinear Analysis of Disk Resonators. Application to Material Characterization and Filter Design.

Jordi Mateu, Carlos Collado, Juan M. O'Callaghan.

Abstract — A procedure for the numerical prediction of the microwave nonlinear behavior (intermodulation products, degradation of quality factors, etc.) of TM_{010} disk resonators has been developed. The procedure is based on relating a very general description of HTS nonlinearities with the circuit elements of a nonlinear radial transmission line. This radial transmission line is then analyzed using the Harmonic Balance algorithm. Successful cross-checks are performed by comparing simulations with theoretical results obtained for a specific model of HTS nonlinearity. The application of this procedure to the determination of nonlinear material parameters from disk resonator measurements is illustrated, as well as its use for simulating filters with several inter-coupled disks.

Index Terms— Disk resonators, filters, intermodulation distortion, nonlinear distortion, superconducting devices.

I. INTRODUCTION

Nonlinear effects in High Temperature Superconducting (HTS) materials may degrade the performance of various types of superconducting devices. HTS filters are most prone to be affected by this type of effects [1]-[4], particularly to the generation of spurious signals like third order intermodulation products. A number of resonator shapes have been proposed to minimize this degradation [5] and, among them, TM_{010} disk resonators are particularly effective [6]. These resonators are also being considered as test structures to determine the nonlinear properties of the HTS material [7], since –as opposed to planar line resonators– the edges do not have a dominant effect in the nonlinear properties of the structure. This removes the uncertainty of possible effects of the etching process, which may damage the edges of the HTS pattern and may have uncontrollable effects on the overall nonlinear properties of the test structure.

In these resonators, the distribution of fields and currents of the fundamental signals can be found by treating the disk as a radial transmission line [7],[8]. This formulation can be extended to treat nonlinear effects and determine the distribution of fields and currents of the spurious signals. This is done in [7], where the third order intermodulation products are found for a TM_{010} disk resonator assuming a specific type of nonlinearity of the HTS material (a square-law dependence of the penetration depth with current density).

In this work we extend the results in [7] to allow other types of HTS nonlinearities. We use a mathematical formulation to describe HTS nonlinearities compatible with that used in [7], but not restricted to a specific dependence of the penetration depth with current density. We find the values of the elements in the nonlinear equivalent circuit of the radial transmission line with our formulation and use the Harmonic Balance algorithm [9] to simulate the nonlinear equivalent circuit of the radial transmission line. This avoids having to do a theoretical analysis to find the amplitude and spatial distribution of spurious signals for each of the plausible models of HTS nonlinearities. This might prove to be an important feature when determining the nonlinear properties of HTS materials, since these properties are known to be strongly dependent on the fabrication process and to change from sample to sample.

Finally, we also illustrate the use of Harmonic Balance to predict the nonlinear performance of HTS filters containing several disk resonators. This prediction is difficult to do analytically regardless of the model used for the HTS nonlinearities, and Harmonic Balance might prove to be a useful and general approach to model high power filters made with superconducting disk resonators.

II. NONLINEAR TRANSMISSION LINE EQUIVALENT OF A DISK RESONATOR

The radial transmission line is described in detail in [8]. This model applies to all the resonant modes with azimuthal symmetry in the disk resonator, and relates the electric ($\mathscr{E}_z$) and magnetic ($\mathscr{H}_\varphi$) fields at a distance ρ from the axis, to currents and voltages through simple equations:

$$v(\rho)=-h\mathscr{E}_z(\rho);\quad i(\rho)=-2\pi\rho\,\mathscr{H}_\varphi(\rho) \tag{1}$$

where h stands for the height of the resonator.

If the dielectric losses are negligible, the voltage and current obey a system of equations similar to the classical transmission line equations:

$$\begin{aligned}\frac{dv}{d\rho} &= -\frac{d}{dt}\left(L_{d0}(\rho)\,i\right)-R_{d0}(\rho)\,i\\ \frac{di}{d\rho} &= -C_d(\rho)\frac{dv}{dt}\end{aligned} \tag{2}$$

with

Manuscript received August 10, 2000.

Authors are with Universitat Politècnica de Catalunya (UPC), Campus Nord UPC D3, Barcelona 08034, Spain. (telephone 34-93-401 7229, email: joano@tsc.upc.es)

This work is supported by the Spanish Ministry of Education and Culture through project MAT-0984-C03-03 and scholarship AP99-78085980 for J. Mateu.

$$L_{d0}(\rho)=\frac{\mu h}{2\pi\rho}+\frac{\mu\lambda(0,T)}{\pi\rho};\ R_{d0}(\rho)=\frac{R_s(0,T)}{\pi\rho}$$
$$C_d(\rho)=\frac{2\pi\rho\varepsilon}{h} \qquad (3)$$

where $\lambda(0,T)$ and $R_s(0,T)$ are the low field values of the penetration depth and surface resistance, and $\lambda(0,T)$ is assumed to be smaller than film thickness t (this constraint affects only the linear part of the problem and could be removed following the steps described in [10]). Note that, in (3), R_{d0} and the term $\mu\lambda(0,T)/\pi\rho$ in L_{d0} account for the resistive and reactive components of the radial electric field at the upper and lower faces of the disk. The radial field component is due to the superconductor and will have components at spurious frequencies if the superconductor behaves nonlinearly. To account for this, the resistance R_{d0} and inductance L_{d0} in (2) should be replaced by current-dependent counterparts R_d and L_d:

$$L_d(\rho,i)=L_{d0}(\rho)+\Delta L_d(\rho,i);\quad \Delta L_d(\rho,0)=0$$
$$R_d(\rho,i)=R_{d0}(\rho)+\Delta R_d(\rho,i);\quad \Delta R_d(\rho,0)=0 \qquad (4)$$

Fig. 1 shows the equivalent circuit of an elemental cell of the radial transmission line. This equivalent circuit also accounts for the nonlinear component of the radial electric field $\mathscr{E}_{nl}$ created by the superconductor, which gives rise to the voltage drop $dv_{nl}=\mathscr{E}_{nl}\,d\rho$. We assume that this field can be expressed as a (nonlinear) function f_{nl} of the surface current density j and its derivatives:

$$\mathscr{E}_{nl}(\rho)=f_{nl}\left(j(\rho),\frac{dj(\rho)}{dt},\frac{d^2j(\rho)}{dt^2},\cdots\right) \qquad (5)$$

with $i=2\pi\rho j$ in a disk resonator. The method of analysis proposed can deal with many possible nonlinear functions f_{nl}. A reasonable form is

$$\mathscr{E}_{nl}(\rho)=a_{nl}(j)\cdot j+\frac{d}{dt}\left[b_{nl}(j)\cdot j\right] \qquad (6)$$

in which the first term in the sum accounts for the nonlinear resistive losses, and the second term quantifies the nonlinearity in the surface reactance. This assumption is compatible with a current-dependent penetration depth postulated in [7], [11]. By using a nonlinear equivalent of the first London equation $(d/dt[\mu_0\lambda(j)j]=\mathscr{E})$ and making $\lambda(j)=\lambda(0,T)(1+f(j))$ with $f(0)=0$ an equivalent value of $b_{nl}(j)$ can be found:

$$b_{nl}(j)=\mu_0\,\lambda(0,T)f(j). \qquad (7)$$

Thus, $b_{nl}(j)$ accounts for the departure of the surface reactance from its small-signal values.

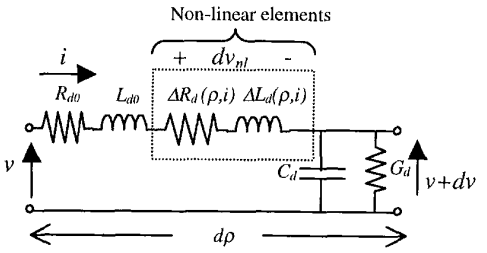

Fig. 1. Elemental cell of a radial transmission line.

Note that in the equations above j denotes surface current density and is related to the volume density j_v through $j=\lambda j_v$.

The distributed parameters $a_{nl}(j)$ and $b_{nl}(j)$, are related to the circuital nonlinear distributed parameters $\Delta R_d(\rho,i)$ and $\Delta L_d(\rho,i)$ in (4) through the following equations:

$$\Delta R_d(\rho,i)=\frac{2a_{nl}(j)}{2\pi\rho}\ ;\ \Delta L_d(\rho,i)=\frac{2b_{nl}(j)}{2\pi\rho}\ ;\ i=2\pi\rho\, j. \qquad (8)$$

Note that other dependences of $\Delta R_d(\rho,i)$ and $\Delta L_d(\rho,i)$ with current density can be derived by postulating particular forms of (5) different than (6).

III. Square-Law Nonlinearities

If the dependence of R_d and L_d with i in (4) can be expressed as a Taylor's series expansion, the lowest-order dependence of R_d and L_d with i is a square-law. This is because (4) has to be even with i. The square-law dependence in (4) is obtained by making $a_{nl}(j)=\Delta r_2\, j^2$ and $b_{nl}(j)=\Delta x_2\, j^2$. Then

$$R_d=R_{do}+\Delta R_2 i^2;\ L_d=L_{do}+\Delta L_2 i^2 \qquad (9)$$

with

$$\Delta R_2=\frac{2\Delta r_2}{(2\pi\rho)^3}\ ;\ \Delta L_2=\frac{2\Delta x_2}{(2\pi\rho)^3}. \qquad (10)$$

Using (9) and following a similar procedure to the one described in [7], we determined the maximum of the current density on the disk as a function of the parameters characterizing the nonlinearities in the HTS material ($\Delta r_2, \Delta x_2$ in our case):

$$J_{2\omega_1-\omega_2}=1.1135\frac{J_1^2J_2^*Q_L}{\omega_0\mu_0 h}(\Delta r_2+j\omega_0\Delta x_2) \qquad (11)$$

where $|J_1|$ and $|J_2|$ are the maximum of the current density at ω_1 and ω_2 ($\omega_1\cong\omega_2\cong\omega_0$) respectively.

The radial distribution of the intermodulation products follows that of the fundamental signals, but their peak value is given by (11). This result will be used to cross-check the application of the Harmonic Balance algorithm, so that it can

TABLE I
CURRENT DENSITIES OF FUNDAMENTAL AND THIRD-ORDER SPURIOUS.

	$\|J_{\omega 1}\|$ A/m	$\|J_{2\omega 1-\omega 2}\|$ A/m
Simulated	251.56	0.1083
Closed-form (11-12)	252.36	0.1099
Error	0.4%	1.5%

These values correspond to the radial positions where currents are maximum. Similar agreement between theoretical and simulated results is found at other radial positions (see Fig. 2).

be used with confidence for other cases where a closed-form solution may not exist (i.e. for $a_{nl}(j)$,$b_{nl}(j)$ not following a square-law with j).

IV. HARMONIC BALANCE. BASICS AND CROSS-CHECK.

The transmission line equivalent allows us to model the disk resonator as a cascade of cells like the one in Fig. 1 and obtain an equivalent circuit with lumped elements, some of which are nonlinear. We can then apply Harmonic Balance algorithms in a similar manner as was done in [12], where the current distributions of fundamental and spurious signals are found for a HTS transmission line. To validate this approach we have simulated the square-law nonlinearities of the preceding section. We have checked the level of intermodulation spurious resulting from the simulation using (11). For the fundamental signals, we have used:

$$Jo = 1.445\sqrt{Po\frac{8\beta}{1+2\beta}Q_L\frac{1}{\omega_0\mu_0 h\pi R^2}} \qquad (12)$$

which gives the peak current density in a two-port, TM_{010} resonator with symmetric coupling. In (12), Po is the available power from the source, β is the coupling coefficient, and R is the radius of the disk.

Table 1 and Fig. 2 show the comparison for a disk with the following features: a 0.5 mm thick dielectric, a 25.4 mm radius, and an unloaded quality factor of 450000. The available power is assumed to be 0.01 W and the couplings are adjusted to obtain a loaded quality factor of 9000. The value of the nonlinear parameter Δx_2, has been chosen to make it consistent with that given in [13] for j_{IMD} (10^7 A/cm^2). To estimate this, an equivalent value of surface current density j_{IMDs} is estimated using $j_{IMDs}=j_{IMD}\cdot\lambda_0$ and (7) is used with $f(j)= 0.5\cdot(j/j_{IMDs})^2$ [13]. The value of Δr_2 is chosen to have the same contribution to the intermodulation current than Δx_2 ($\Delta r_2= \omega_0\cdot\Delta x_2$, see (11)). The resulting values are: $\Delta x_2=3\text{x}10^{-22}$ (H m^2)/A^2 and $\Delta r_2=2.8\text{x}10^{-12}$ (Ω m^2)/A^2.

V. PREDICTION OF FILTER PERFORMANCE BASED ON ADJUSTMENT OF EXPERIMENTAL MEASUREMENTS.

Harmonic Balance is an efficient algorithm that makes fast simulations given $a_{nl}(j)$ and $b_{nl}(j)$. The speed of simulations allows for an iterative adjustment of $a_{nl}(j)$ and $b_{nl}(j)$ to fit the simulation results with experimental data. Disk resonators are especially suitable for this since (8) sets a very simple relation between the material parameters $a_{nl}(j)$ and $b_{nl}(j)$ and

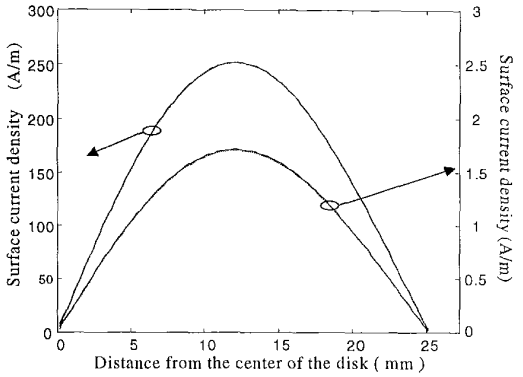

Fig. 2. Radial distribution of current densities for the fundamental (left scale) and third order (right scale) intermodulation currents. Plots show overlapped traces with simulated vs. theoretical results.

the parameters of the equivalent transmission line. This does not happen in planar transmission line resonators.

To illustrate this, we have used the experimental data presented in [14]. The linear elements of the transmission line equivalent (L_{d0}, R_{d0} and C_d) have been inferred from the small signal measurements and the geometry of the resonators using (3). The current-dependent elements ($\Delta R_d(\rho,i)$ and $\Delta L_d(\rho,i)$) have been adjusted to match dependence of the power of the intermodulation products with that of the source. This dependence has a 2:1 slope which can be matched in the simulations by making $a_{nl}(j)=\Delta r_a|j|$ and $b_{nl}(j)=\Delta x_a|j|$.

The resulting transmission line parameters are:

$$R_d = R_{do} + \Delta R_a|i|\,;\, L_d = L_{do} + \Delta L_a|i| \qquad (13)$$

with

$$\Delta R_a = \frac{2\Delta r_a}{(2\pi\rho)^2}\;;\Delta L_a = \frac{2\Delta x_a}{(2\pi\rho)^2}\,. \qquad (14)$$

Fig. 3 shows the simulation results obtained with $\Delta r_a=2.9\text{x}10^{-13}$ (Ω m)/A and $\Delta x_a= 0$. There is a continuum of Δr_a ,Δx_a pairs, capable of reproducing Fig. 3, depending on how much nonlinearity is attributed to the resistive and reactive parts of the surface impedance, and an almost identical figure is obtained at the opposite extreme using

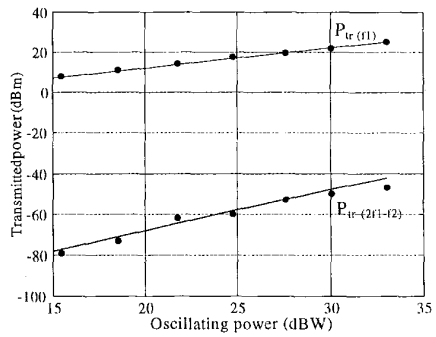

Fig. 3. Fundamental and third order intermodulation transmitted power vs. Oscillating power. These simulated data (lines) reproduce the measurements made in [14] (circles)

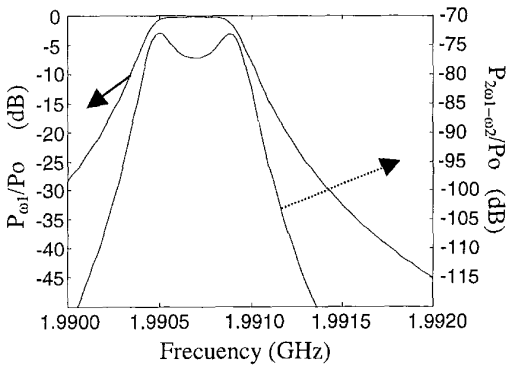

Fig. 4. Frequency response of a three-pole TM_{010} disk filter. Left vertical scale corresponds to the fundamental signal. Right vertical scale corresponds to the of intermodulation product when the fundamental signals are swept with a constant frequency difference of 1KHz. Source power is 10 dBm per carrier.

Δr_a=0 and Δx_a=1.223x10^{-19} (H m) /A. Other observables (like the degradation of the quality factor, or the change in the resonant frequency with the source power) are necessary to discern this. In our case, a degradation of the quality factor with source power similar to that obtained in [14] is obtained with the first pair of Δr_a ,Δx_a values.

Once a transmission line equivalent of the disk resonator is available, a circuit simulation containing several coupled disks can be set-up. As an example, a three pole bandpass filter has been designed following standard techniques [15] and simulated using our code and the values of Δr_a ,Δx_a found above. The output data from this simulation can be displayed in several forms. For example, Fig. 4 shows the frequency dependence of the intermodulation product superimposed to the frequency response of the filter. This figure shows intermodulation peaks at the edges of the bandpass, in good qualitative agreement with other results [16], [17]. Other possible outputs of the simulator include an equivalent of Fig. 3, and the spacial distribution of fundamental and spurious currents in all the filter resonators as a function of frequency.

VI. Conclusions

A general method has been proposed to relate the nonlinearities of the HTS material to the parameters of an equivalent circuit of a HTS TM_{010} resonator. It has been shown that this circuit can be properly simulated using Harmonic Balance. This approach has been shown to be promising for the determination of the HTS nonlinear parameters from experimental measurements, since there are simple equations that relate the material parameters with the elements of the equivalent circuit being fitted. Harmonic Balance has also been shown to be useful for the simulation of filters containing several disk resonators.

Acknowledgment

The authors want to acknowledge Salvador Talisa for helpful comments and suggestions.

References

[1] D. E. Oates, A.C. Anderson, D.M. Sheen and S.M.Ali, "Stripline resonator measurements of Zs versus H_{rf} in Y Ba Cu O thin films" *IEEE Trans. On Microwave Theory and Techniques,* vol. 39, no. 9 pp. 1522-1529, Sept. 1991

[2] P.P Nguyen, D.E. Oates, G. Dresselhaus, M.S. Dresselhaus, "Nonlinear surface impedance for $Yba_2Cu_3O_{7-x}$ thin films: Measurements and a coupled-grain model", *Physical Review B*, vol. 48, no. 9 pp 6400-6413, 1993.

[3] J.H. Oates, R.T. Shin, D.E. Oates, M.J Tsuk, P.P. Nguyen, "A nonlinear transmission line model for superconducting stripline resonators", *IEEE Transactions on Applied Superconductivity*, vol. 3, no. 1, pp. 17-22, 1993.

[4] B. Avenhaus, A.Porch, M.J Lancaster, et. al, "Microwave properties of YBCO thin films", *IEEE Transactions on Applied Superconductivity,* vol. 5, no. 2, pp 1737-1740, June 1995.

[5] Z-Y. Shen, C. Wilker, P. Pang, D.W. Face. C. F. Carter. C. M. Harrington, "Power handling capability improvement of high-temperature superconducting microwave circuits", *IEEE Transactions on Applied Superconductivity,* vol. 7, no. 2, pp. 2446-2543, June 1997.

[6] H. Chaloupka, M. Jeck, B. Gurzinski, S. Kolesov, "Superconducting planar disk resonators and filters with high power handling capability", *Electon.Lett.,* vol. 32, no. 18, pp. 1735-1736, August 1996.

[7] T. Dahm, D.J. Scalapino and B.A. Willemsen, "Microwave intermodulation of a superconducting disk resonator", *J. Appl. Phys.*, vol. 86, no. 7, pp.4055-4058, Oct. 1999.

[8] S. Ramo, J.R. Whinnery and T. Van Duzer, *Fields and Waves in Communication Electronics*, John Wiley & Sons, inc., 1994.

[9] S. A. Maas, *Nonlinear Microwave Circuits* , Artech House, 1988.

[10] L.H. Lee, W.G. Lyons, T.P. Orlando, S.M. Ali, R.S. Withers, "Full-wave analysis of superconducting microstrip lines on anisotropic substrates using equivalent surface approach", *IEEE Transactions on Applied Superconductivity,* vol. 41, no. 12, pp 2359-2367, Dec. 1993.

[11] B.A. Willemsen, T. Dahm, B.H.King and D.J. Scalapino, "Microwave intermodulation in high-Tc superconducting microstrip resonator", *IEEE Transactions on Applied Superconductivity*, vol 9, no. 2 pp 4181-4184, June 1999

[12] C. Collado, J. Mateu, J.M. O'Callaghan, "Computer simulation of the non-linear response of superconducting devices using the Multiport Harmonic Balance algorithm", *Inst. Of Phys. Conf. Ser. No.* 167, pp 411-414, 2000.

[13] R.B. Hammond, E.R.Soares, B.A. Willemsen, T.Dahm, D.J.Scalapino and J.R. Schirieffer, "Intrinsic limits on the Q and intermodulation of low power high temperature superconducting microstrip resonator", *J. Applied Physics*, vol. 84, no. 10, pp. 5662-5667, 1998.

[14] S.Kolesov, H. Chaloupka, A. Baumfalk and T. Kaiser, "Planar HTS structures for high power applications in communications systems," *J Superconductivity,* vol. 10, no. 3, pp. 179-187, 1997

[15] G.L. Matthaei, L.Young and E.M.T. Jones, *Microwave filters, impedance matching networks and coupling structures*, Mc Graw-Hill Book Company, 1964

[16] T. Yoshitake, S Tahara and S. Suzuki, "Intermodulation distortion measurements of microstrip band-pass filter made from double-sided YBaCuO films", *Appl.Phys. Lett.*, vol. 67, no. 26, pp. 3963-3965, 1995.

[17] T. Dahm and D.J. Scalapino, "Analysis and Optimization of Intermodulation in High-Tc Superconducting Microwave Filter Design", *IEEE Transactions on Applied Superconductivity*, vol. 8, no.4, pp.149-157, Dec 1998